J. Nanoanalysis., 7(2): 152-165, Spring 2020

RESEARCH ARTICLE

Synergistic effects of Titanium dioxide nanoparticles and Paclitaxel combination on the DNA structure and their antiproliferative role on MDA-MB-231cells

Azadeh Hekmat[1*], Masoumeh Afrough[1], Saeed Hesami Tackallou[2], Faizan Ahmad[3]

[1] Department of Biology, Science and Research Branch, Islamic Azad University, Tehran, Iran

[2] Department of Biology, Central Tehran Branch, Islamic Azad University, Tehran, Iran

[3] Centre for Interdisciplinary Research in Basic Sciences, Jamia Millia Islamia, New Delhi, India

ARTICLE INFO

Article History:
Received 2019-05-20
Accepted 2020-02-16
Published 2020-05-01

Keywords:
Titanium dioxide nanoparticles (TiO_2NPs)
Paclitaxel (PTX)
Spectroscopy
C-form DNA
MDA-MB-231cells

ABSTRACT

Objective(s): The objective of this investigation was to evaluate the synergistic effect of paclitaxel (PTX) combined with titanium dioxide nanoparticles (TiO_2NPs) on DNA structure and to examine the proliferation of MDA-MB-231cells.

Methods: This investigation performed with Ultraviolet spectroscopy, zeta potential investigation, circular dichroism (CD) spectroscopy, ELISA reader and fluorescence spectroscopy.

Results: The Ultraviolet results indicated that the structure of DNA in the presence of PTX and TiO_2NPs (at a lower concentration) changed significantly rather than TiO2NPs or PTX alone. The fluorescence results exposed that PTX+TiO_2NPs could form a complex via non-intercalative mechanism and the PTX+TiO_2NPs affinity to DNA increased considerably. The thermodynamics parameters displayed that PTX+TiO_2NPs interact with DNA strongly and in this interaction, the hydrophobic force plays an important role. The CD data confirmed that DNA structure was modified by PTX+TiO_2NPs via a simple and reasonable mechanism: change in DNA conformation from B to C-form. The negative charge of DNA reduced strongly after addition of PTX+TiO_2NPs. The anticancer property of PTX+TiO_2NPs by MTT assay demonstrates that this combination can tremendously diminish the proliferation of MDA-MB-231cells compared to PTX or TiO_2NPs alone.

Conclusions: Based on this investigation TiO_2NPs could enhance the affinity and binding of PTX (at a lower concentration) on DNA structure and PTX+NDs can promote mortality of MDA-MB-231 cells. This study can offer an innovative strategy for designing the ideal anti-tumor agents.

How to cite this article
*Hekmat A., Afrough M., Hesami Tackallou S., Ahmad F. Synergistic effects of Titanium dioxide nanoparticles and Paclitaxel combination on the DNA structure and their antiproliferative role on MDA-MB-231cells. J. Nanoanalysis., 2020; 7(2): *152-165. DOI: 10.22034/JNA.2020.1869287.1141.*

INTRODUCTION

Among semiconductor nanoparticles (NPs), the titanium dioxide nanoparticles (TiO_2NPs) are being widely consumed in the nanotechnology industry in regard to high stability, anti-rust, chemical ineffectiveness, photocatalytic properties, and strong oxidizing properties [1]. TiO_2NPs can be found in many products, e.g., food additives, environmental decontamination systems, and cosmetics [2]. Numerous investigations have displayed that TiO_2NPs can initiate genotoxicity and cytotoxicity [3, 4].

Needles of yew trees, *Taxus baccata*, produce an anti-tumor agent called Paclitaxel (PTX). Since PTX has the property to bind DNA and can affect cell division, this natural product is commonly utilized in chemotherapeutic agents [5]. In 1992, the FDA (the United States Food and Drug Administration) approved PTX under the brand name Taxol® [6].

* Corresponding Author Email: *hekmat@ut.ac.ir*

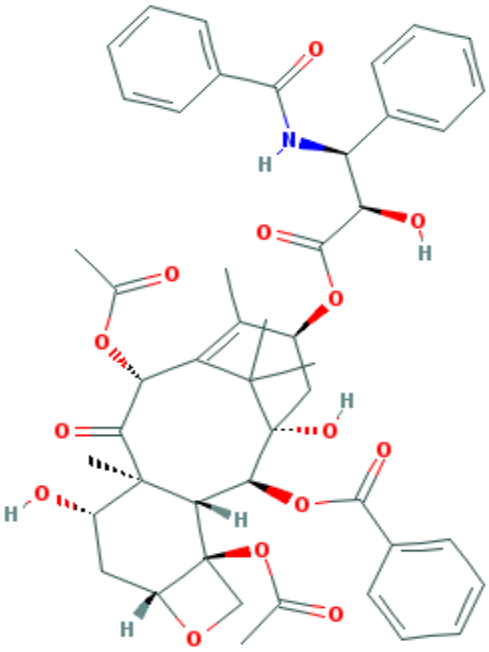

Fig. 1. The Paclitaxel (PTX) chemical structure.

Ouameur *et. al.* showed taxol interact with DNA with two different binding types [6]. Despite a good clinical ability exhibited via PTX, there is still a growing need to attain a better pharmacokinetic profile for PTX.

DNA is often employed as a target for cancer therapy. The investigation of DNA and small molecule interaction is important and exciting not only in realizing the interaction mechanism but also for the innovative medicines design. Numerous reports indicate that the combination of several anticancer drugs can reduce the side effects of a single drug with a high dose [7, 8]. Some studies explored the effects of surface-modified of PTX with TiO_2NPs *in vivo* and *in vitro*. For example, Venkatasubbu *et. al.* discovered that the PTX with modified surface attached TiO_2NPs and hydroxyapatite had a higher anticancer activity compare with the pure PTX [9]. Nevertheless, the goal of this research is to discover the synergistic anti-malignancy effect of PTX combined with TiO_2NPs on DNA structure. To the best of our acquaintance, there is not considerable research about the synergistic anti-tumor effect of PTX combined with TiO_2NPs on DNA structure in physicochemical terms. Regardless of many new formulations in the PTX market, none of them has 100% efficiency and many of them have numerous adverse effects. Recently, a number of advanced nano-formulations of PTX have been developed with the purpose of enhancing the efficiency of PTX. The present study is designed to offer an essential understanding of the interaction mechanism between PTX+TiO_2NPs with DNA in detail using multiple spectroscopic instruments. The objective of this research is to evaluate the synergistic effects of PTX combined with TiO_2NPs on DNA structure. Although further investigations are required, this study can provide a novel strategy for designing the ideal PTX formulation, i.e. enhancing tumor uptake and improving the PTX bio-distribution.

MATERIALS AND METHODS

Materials

Chemicals: DNA from calf thymus (lyophilized powder), TiO_2NPs (Anatase phase, powder, less than 10 nanometers, 99% of purity, special surface area 150 m^2/g), Paclitaxel (Fig. 1) and Dimethylthiazol-2-yl]-2, 5-diphenyltetrazolium bromide (MTT) were acquired from Sigma Aldrich Co. (USA), Pars Lima Co. (Iran) and Stragen Pharma Co. (Switzerland), respectively. TiO_2NPs were diluted with deionized water, sonicated for uniform suspension (10 minutes) then stored at 4 °C. Ethidium Bromide and Tris(hydroxymethyl) aminomethane (Trizma® base) were achieved

from Merck Co. (USA) and Sinagen Co. (Iran). The MDA-MB-231 human breast cancer cell line was obtained from the National Cell Bank of Iran, Pasteur Institute, Iran. The Trypsin-EDTA, streptomycin, RPMI 1640, fetal bovine serum (FBS), and penicillin were prepared from Gibco, USA. Dimethylsulfoxide (DMSO) was obtained from Merck, Germany. All experiments were done in Tris-base buffer (pH 7.4, 0.1 M) and deionized (DI) double-distilled water (ER 18.3 mΩ), was utilized.

Devices: Ultraviolet-visible spectrophotometer CARY, 100 Conc, (UK), Varian Cary Eclipse Fluorescence Spectrophotometer (USA), Aviv Circular Dichroism Spectrometer model 215 (USA), Zetasizer Nano-ZS model Malvern, (UK), the ELISA reader model Expert 96, Asys Hitech (Austria) and Thermo Scientific Barnstead NANOpure (USA) were utilized. All results are representative of three independent experiments.

Methods

Ultraviolet (UV) Absorption Measurements

Firstly, the UV–Vis spectra of DNA solution (8.32 μM) upon addition of different amounts of TiO_2NPs (3.1-46.5 μM) and PTX (17.5-160 μM) were obtained. In the next experiment, various amounts of TiO_2NPs (3.1-18.6 μM) were added to a cuvette filled with the DNA solution (8.32 μM) and 60 μM of PTX (amount at the half-saturation of PTX+DNA), and then UV spectral changes were monitored. In another experiment, a fixed amount of TiO_2NPs (15.5 μM) was added to 60 μM of PTX and then UV spectral changes were monitored. All experiments were run and verified in a 1 cm quartz cell thermostated at 37°C. The solution was thoroughly mixed during the period of titration.

Fluorescence Measurements

At first, TiO_2NPs at a concentration range of 3.1-46.5 μM were added to the DNA-EtBr solution and fluorescence measurements were done at 27 and 37 °C. Then, different amounts of PTX (17.5-755 μM) were added into the DNA-EtBr solution and fluorescence measurements were carried out at 27 and 37 °C. Subsequently, various concentrations of TiO_2NPs (3.1-37.2 μM) were added to the DNA-EtBr-PTX mixture and fluorescence intensities were taken at 27 and 37 °C. The excitation wavelength was 475 nm and the emission wavelength was 604 nm. In all experiments, a 5 nm emission and excitation slits and a cuvette with a 1 cm path length were used. The concentrations of DNA and EtBr were 8.32 μM and 0.72 μM, respectively. For inner filter effect correction caused by the attenuation in excitation and emission signal producing from the quencher absorption, Eq. 1 was used [10]:

$$F_{corr} = F_{obs}.10^{(Ab_{ex}+Ab_{em})/2} \quad (1)$$

Where $Ab_{ex,}$ Ab_{em} F_{corr}, and F_{obs}, are the mixture absorption at the excitation wavelength, the mixture absorption at emission wavelength, the corrected fluorescence intensities, and the fluorescence intensities, respectively [10].

Circular Dichroism (CD) Measurements

By adding TiO_2NPs (46.5 μM), PTX (160 μM) and PTX (60 μM)+TiO_2NPs (15.5 μM) to DNA (8.32 μM) the CD spectra were assessed in the wavelength range of 220-320 nm by means of a quartz cell, a path length of 0.1 cm, with a 0.2 nm resolution and 20 nm min^{-1} speed scanning at 37 °C. These concentrations were acquired from ultraviolet absorption measurements. The DNA solution was saturated when 46.5 μM of TiO_2NPs or 160 μM of PTX were added. Furthermore, the DNA solution was half saturated at 60 μM of PTX.

Zeta-Potential (z) Measurements

First, the DNA ζ-potential values in the absence and presence of PTX and TiO_2NPs were evaluated. The concentrations of TiO_2NPs and PTX were 46.5 μM and 160 μM, respectively. Subsequently, the ζ-potential of DNA was explored by adding PTX (60 μM)+TiO_2NPs (15.5 μM) at 37 °C. The Zeta-potential average values were achieved with the data from four runs.

Cells and Cell Culture

The human breast cancer cell line MDA-MB-231 (ATCC® HTB-26™, USA) was maintained in RPMI 1640 medium, containing 2 mM L-glutamine, 5 μg/mL penicillin and streptomycin, and 10% heat-inactivated FBS in a 5% CO_2 humidified atmosphere incubator at 37 °C. The cells were grown routinely as monolayer culture.

MTT assay

The MDA-MB-231 cells in the log phase were trypsinized and seeded in 96-well plates. The medium of each well was replaced by a fresh medium after 48 h of incubation with different concentrations of sterilized TiO_2NPs (5, 10, 20, 40,

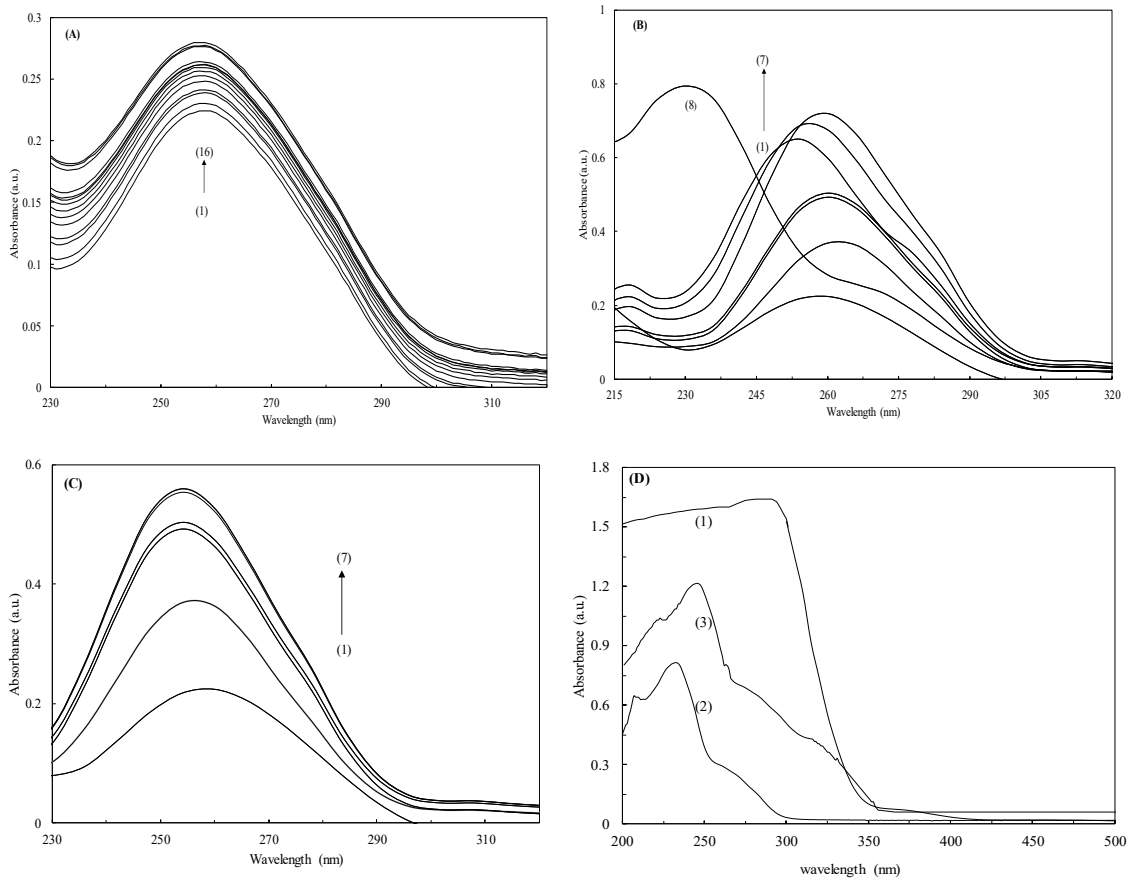

Fig. 2. Absorption spectra of: (A) DNA (1) with increasing concentrations of TiO_2NPs (2-16); (B) DNA (1) with increasing concentrations of PTX (2-7) and PTX alone (8); (C) DNA (1), DNA+PTX (2) and DNA+PTX with increasing concentrations of TiO_2NPs (3-7); (D) TiO_2NPs alone (1), PTX alone (2) and TiO_2NPs+PTX (3) at 37 °C.

80, 100 and 200 µM) and sterilized PTX (0.2, 0.3, 0.4, 0.5, 0.6, 0.7 and 0.8 µM). The cells were also incubated with 0.4 and 0.5 µM PTX in combination with 20, 40, and 60 µM TiO_2NPs (concentrations were chosen according to MTT assay results). Subsequently, 20 µL MTT (5 mg/mL in PBS buffer) was added into each well and incubated for 3 h at 37 °C. Later, the insoluble formazan formed was dissolved in 100 µl of DMSO (Dimethyl sulfoxide). The optical density (OD) of each well, was calculated against reagent blank with ELISA reader at 490 nm. Each experiment was repeated 3 times, in addition for each concentration performed in triplicate format.

RESULTS

UV Absorption Investigations

The characterizing absorption peak (λ_{max}) of DNA is at 260 nm. This λ_{max} is caused by the chromophoric groups in pyrimidine and purine moieties accountable for the electronic transitions and these transitions probabilities are high [5]. As exhibited in Fig. 2A, upon subsequent addition of TiO_2NPs to the solution of DNA at 37 °C, hyperchromism is observed, demonstrating the formation of a complex between DNA and TiO_2NPs. As shown in Fig. 2B with the increase of PTX concentration, the absorption bond of DNA increased continuously, which displayed a λ_{max} around 254 nm. Since PTX was added to both cuvettes and the UV spectrum of PTX alone displayed a λ_{max} around 230 nm (Fig. 2B), the increment in absorbance is the result of the complex formation between DNA and PTX. Finally, 60 µM of PTX (amount at the half-saturation of PTX+DNA) was added to the solution of DNA followed by titration of TiO_2NPs into the mixture and reference cuvette (Fig. 2C). With the addition of TiO_2NPs to DNA+PTX solution hyperchromic

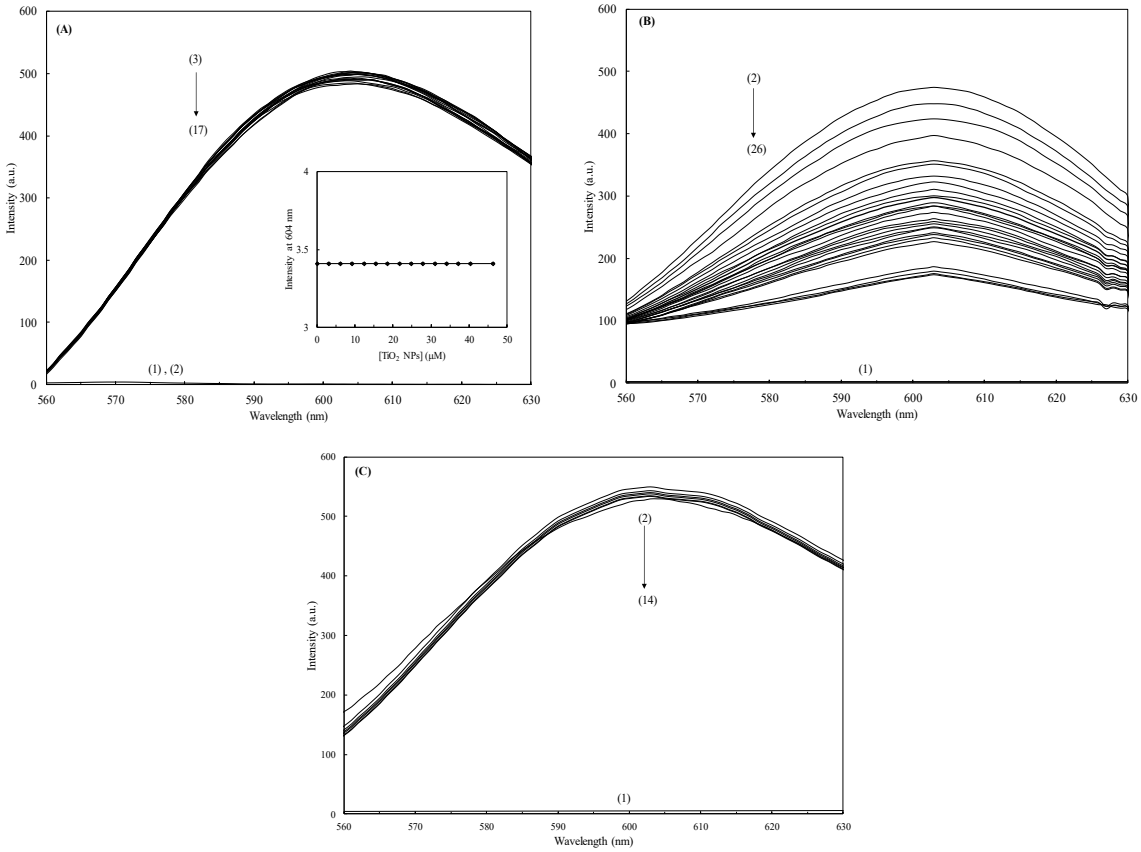

Fig. 3. The fluorescence emission spectra of: (A) DNA intercalated with EtBr after adding various concentrations of TiO_2NPs; the fluorescence emission of DNA alone (1), TiO_2NPs alone (2), DNA-EtBr (3) and the fluorescence quenching with increasing concentrations of TiO_2NPs (4-17) are shown. The inset shows the EtBr fluorescence intensity upon addition of TiO_2NPs; (B) DNA intercalated with EtBr after increasing concentrations of PTX; the fluorescence emission of PTX alone (1), DNA-EtBr (2), and the fluorescence quenching with increasing concentrations of PTX (3-26) are shown; (C) DNA intercalated with EtBr and fixed concentration of PTX with increasing concentrations of TiO_2NPs; the fluorescence emission of DNA alone (1), DNA-EtBr (2), DNA-EtBr-PTX (3) and the fluorescence quenching by increasing concentrations of TiO_2NPs (4-14) are shown.

in absorbance occurred and was along with a blue shift in λ_{max}, which indicates the interaction between TiO_2NPs to DNA+PTX.

In the next study, a fixed amount of TiO_2NPs was added to 60 μM of PTX (Fig. 2D). In the presence of TiO_2NPs, a rising trend in λ_{max} of PTX was found.

Fluorescence Intensity Investigations

DNA and TiO_2NPs alone have no fluorescence emission in the (Fig. 3). In the presence of DNA, Ethidium Bromide (EtBr), the DNA fluorescent probe, has an extreme fluorescence emission spectrum with a $\lambda_{max,em}$ at 604 nm. Accordingly, at first, the characteristic alterations in fluorescence emission spectra were clarified at titration of TiO_2NPs with DNA-EtBr solution (Fig. 3A). The intensity of DNA-bound EtBr was decreased with increasing concentrations of TiO_2NPs without any shifts in fluorescence $\lambda_{max,em}$. The fluorescence emission spectra of DNA-EtBr in the absence and presence of PTX were shown in Fig. 3B. Through increasing the PTX concentration, fluorescence quenching occurred gradually with no shifts in fluorescence $\lambda_{max,em}$. In the next step, fluorescence titration was achieved for the DNA-EtBr-PTX solution with increasing TiO_2NPs (Fig. 3C). Through increasing the concentration of TiO_2NPs fluorescence quenching took place with no shifts in fluorescence $\lambda_{max,em}$.

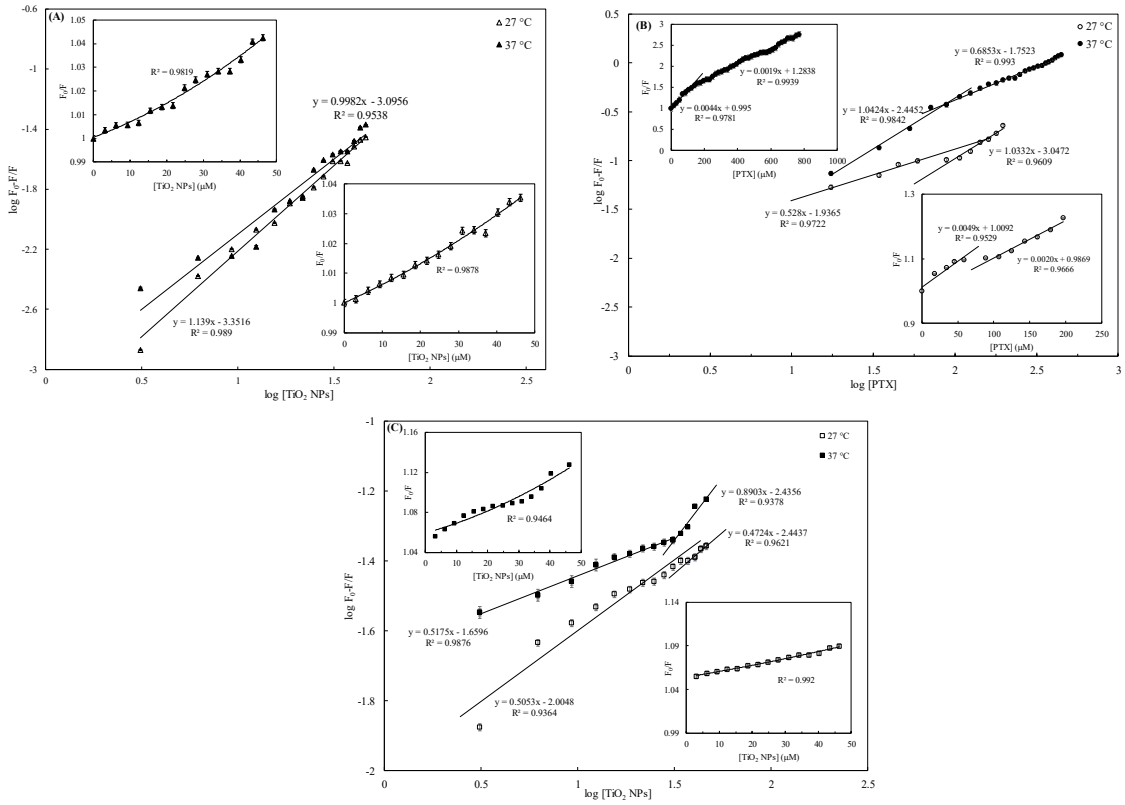

Fig. 4. The Modified Stern-Volmer plot of DNA-EtBr in the presence of various concentrations of (A) TiO_2NPs, (B) PTX and (C) PTX+TiO_2NPs at 27 and 37 °C. The Insets display the Stern–Volmer plot of DNA-EtBr in the presence of numerous concentrations of (A) TiO_2NPs, (B) PTX and (C) DNA-EtBr-PTX in the presence of diverse concentrations of TiO_2 NPs at 27 and 37 °C. The data are obtained from the Means of three independent measurements.

The Quenching Mechanisms

The data of fluorescence quenching for TiO_2NPs-DNA, PTX-DNA, and TiO_2NPs-PTX-DNA were fitted to the Stern-Volmer equation (Eq. 2) [10]:

$$\frac{F_0}{F} = 1 + K_{SV}[Q] = 1 + k_q \tau_0 [Q] \quad (2)$$

In this equation, F and F_0 were the fluorescence data in the presence of TiO_2NPs or PTX and the fluorescence data in the absence of TiO_2NPs or PTX, respectively. t_0, and [Q] were the EtBr lifetime in the excited state (23 ns) and the concentration of TiO_2NPs or PTX, respectively. k_q and K_{SV} were the bio-molecular quenching constant and the Stern-Volmer dynamic quenching value constant, respectively [10]. By means of Eq. 2, a linear plot for F_0/F versus [PTX] at 27 and 37 °C was acquired (Insets of Fig. 4B). With the Stern-Volmer plot, we have calculated K_{SV1}=4.4×10^3 M^{-1}, K_{SV2}=1.9×10^3 M^{-1}, k_{q1}=2.0×10^{12} M^{-1} s$^{-1,}$ and k_{q2}=8.6×10^{12} M^{-1} s^{-1}, i.e. DNA has two binding constants for PTX. Dynamic (collisional) and complex formation (static) quenching can be determined by means of determining the temperature dependence of the fluorescence quenching. As displayed in the inset of Fig. 3B, K_{SV} for DNA-EtBr with PTX decreased from 4.9×10^3 and 2×10^3 M^{-1} to 4.4×10^3 and 1.9×10^3 M^{-1} at the increasing temperature from 27 to 37 °C. In contrast, consistent with Eq. 2, a positive deviation for the plots of F_0/F vs. [TiO_2NPs] at 27 and 37° C were achieved (Insets of Fig. 4A and C).

Determination of the Binding Constants (K_A) and the Binding Sites (n)

Supposing that there were similar and independent binding sites in DNA–EtBr, with Eq. 3, K_A and n were calculated [1]:

$$\log \frac{F_0 - F}{F} = \log K_A + n \log[Q] \quad (3)$$

Table 1. The K_A (binding constants), n (number of binding sites) and ΔG° of DNA in the presence of TiO_2NPs, PTX and PTX+TiO_2NPs at 37° C.

Sample	27 °C			37 °C		
	K_A (M^{-1})	n	ΔG° (kJ mol^{-1})	K_A (M^{-1})	n	ΔG° (kJ mol^{-1})
DNA+TiO_2NPs	4.4×10^2	1.2	-15.2	8.0×10^2	0.9	-17.2
DNA+PTX	8.9×10^2	1.03	-16.9	3.6×10^3	1.0	-21.1
	1.6×10^4	0.6	-24.1	1.7×10^4	0.7	-25.1
DNA+PTX+TiO_2NPs	3.6×10^3	0.6	-20.4	4.0×10^3	0.9	-21.4
	9.0×10^3	0.5	-22.7	2.1×10^4	0.5	-25.7

Table 2. Thermodynamic parameters for the binding of TiO_2 NPs, PTX and PTX+ TiO_2 NPs to DNA.

Sample	300 K	310 K		
	ΔG° (kJ mol^{-1})	ΔG° (kJ mol^{-1})	ΔH° (kJ mol^{-1})	ΔS° (J mol^{-1} k^{-1})
DNA+TiO_2NPs	-15.2	-17.2	46.2	204.7
DNA+PTX	-16.9	-21.1	108.1	416.6
	-24.1	-25.1	4.7	96.1
DNA+PTX+TiO_2NPs	-20.4	-21.4	8.1	95.2
	-22.7	-25.7	65.5	294.1

Apparently, by plotting $\log\frac{F_0-F}{F}$ against log [Q], the K_A and n could be determined. Consistent with Fig. 4, K_A and n for TiO_2NPs-DNA, PTX-DNA and TiO_2NPs-PTX-DNA were achieved, respectively. It could be realized that the plots exhibited a good linear relationship. The binding data arise from Eq. 3, and they are demonstrated in Table 1. At different temperatures, the values of K_A are different.

The Determination of the Binding Forces

Applying K_A, the ΔG^0 (the change in standard free energy) can be determined by the following equation [10]:

$$\Delta G^\circ = -RT\ln K \quad (4)$$

Where T and R are the absolute temperature and the universal gas constant, respectively. In Table 2 the magnitudes of ΔG^0 were summarized. The thermodynamic parameters, ΔH° (enthalpy change) and ΔS° (entropy change) are the main components to determine the model of interaction between TiO_2NPs, PTX and PTX+TiO_2NPs and DNA. By using the Van't Hoff equation (Eq. 5), ΔH° and ΔS° were calculated [11]:

$$\ln k = \frac{-\Delta H^\circ}{R}\frac{1}{T} + \frac{\Delta S^\circ}{R} \quad (5)$$

The positive ΔH° and ΔS° values in Table 2 specify that hydrophobic force plays the most important role in the TiO_2NPs, PTX, and PTX+TiO_2NPs and DNA binding interactions [11].

Circular Dichroism (CD) Investigations

As presented in Fig. 5, the spectrum of DNA in B form has two absorbing peaks: a negative ellipticity at 245 nm (first) and a positive ellipticity at 275 nm (second), which are related to a right-handed chiral structure and base stacking, respectively [11]. In comparison with free DNA, after TiO_2NPs, PTX, or PTX+TiO_2NPs addition, the DNA solution still preserves basic CD spectrum shape, however its negative band as well as positive band increase and decrease, respectively (Fig. 5). For negative ellipticity at 245 nm band, the order (from bottom to top) is DNA+PTX+TiO_2NPs> DNA+PTX> DNA+TiO_2NPs> DNA, and for positive ellipticity at 275 nm band, the order (from top to bottom) is DNA ≅ DNA+TiO_2NPs> DNA+PTX> DNA+PTX+TiO_2NPs.

Zeta-potential (z) Investigations

The free DNA ζ-potential was found to be about −24.06 mV. This value is consistent with the earlier report [12]. As seen in Table 3, the ζ-potential of DNA reduced after addition of TiO_2NPs (−19.78 mV) and PTX (−18.55 mV). Nevertheless, the ζ-potential of DNA reduced significantly from the original −24.06 mV to −16.14 mV after addition of PTX in combination with TiO_2NPs.

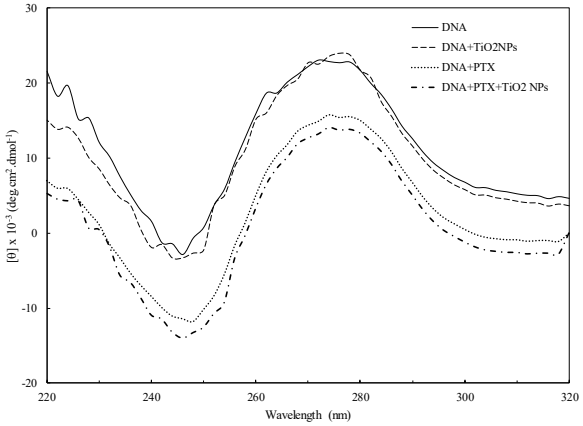

Fig. 5. The CD spectra of DNA in the absence and presence of TiO_2NPs, PTX, and PTX+TiO_2NPs at 37° C.

Table 3. Zeta-potentials of DNA in the absence and presence of TiO_2NPs, PTX and PTX+TiO_2NPs at 37° C.

Sample	ζ-potential (mV)
DNA	–24.06
DNA-PTX	–18.55
DNA-TiO_2 NPs	-19.78
DNA-TiO_2 NPs-PTX	-16.14

The growth rate of MDA-MB-231 cells

The effects of diverse concentrations of TiO_2NPs and PTX were examined in MDA-MB-231 cells after incubation for 48 h. As shown in Fig. 6A, B, TiO_2NPs alone, and PTX alone reduced the viability of MDA-MB-231 cells. The IC_{50} (50% inhibition concentration) of PTX alone and TiO_2NPs alone were determined to be 0.65 and 90 µM. Then, by the use of MTT assay, PTX was employed at concentrations of 0.4 µM and 0.5 µM, combined with TiO_2NPs at the concentrations of 20, 40, and 60 µM to attain the optimum combination condition that affected the majority of MDA-MB-231 cells (Fig. 6C).

DISCUSSION

Several reports specify that the combination of several anticancer drugs can reduce the side effects of a single drug with a high dose. DNA molecule is the pharmacological target of numerous drugs. In this study, fluorescence spectroscopy, UV spectroscopy, zeta-potential study, and CD spectroscopy have been applied to monitor the conformation changes of DNA induced by paclitaxel combined with TiO_2NPs. The study of small ligands–DNA interactions could be carried out via UV absorption spectroscopy by monitoring any variations in the maximum absorption (λ_{max}) of the DNA molecule. Upon subsequent addition of TiO_2NPs to the solution of DNA, hyperchromism is detected, signifying a complex formation between DNA and TiO_2NPs (Fig. 2A). The hyperchromism was also attributable to pyrimidine and purine bases exposure [1]. Vujčić *et. al.* [17] proposed that the negatively charged of DNA could interact with positively charged of TiO_2NPs and one of the oxygen atoms of titanium dioxide can release as a ROS (reactive oxygen species) resulting in DNA damage. Therefore, based on our results and previous reports [13, 14], it can be hypothesized that TiO_2NPs modifies DNA structure by a simple and reasonable mechanism: interact with the phosphate backbone of DNA and release ROS. With the increment of PTX concentration, the absorption band of DNA increased continuously, which displayed a λ_{max} around 254 nm (Fig. 2B). Our UV spectrum of PTX alone is in agreement with the previous study [15]. The observed hyperchromism and a blue shift (from 260 nm to 254 nm) suggested that PTX strongly binds to DNA owing to groove binding [11] and consequently causing DNA secondary structure destruction [16]. Additionally, the absorption intensity was increased attributable to the fact that pyrimidine and purine bases of DNA are exposed [17]. This result is in agreement with the previous study, which displayed that PTX binds to the DNA major and minor grooves [6, 18]. Interaction with compounds could change the absorbance intensity and the value

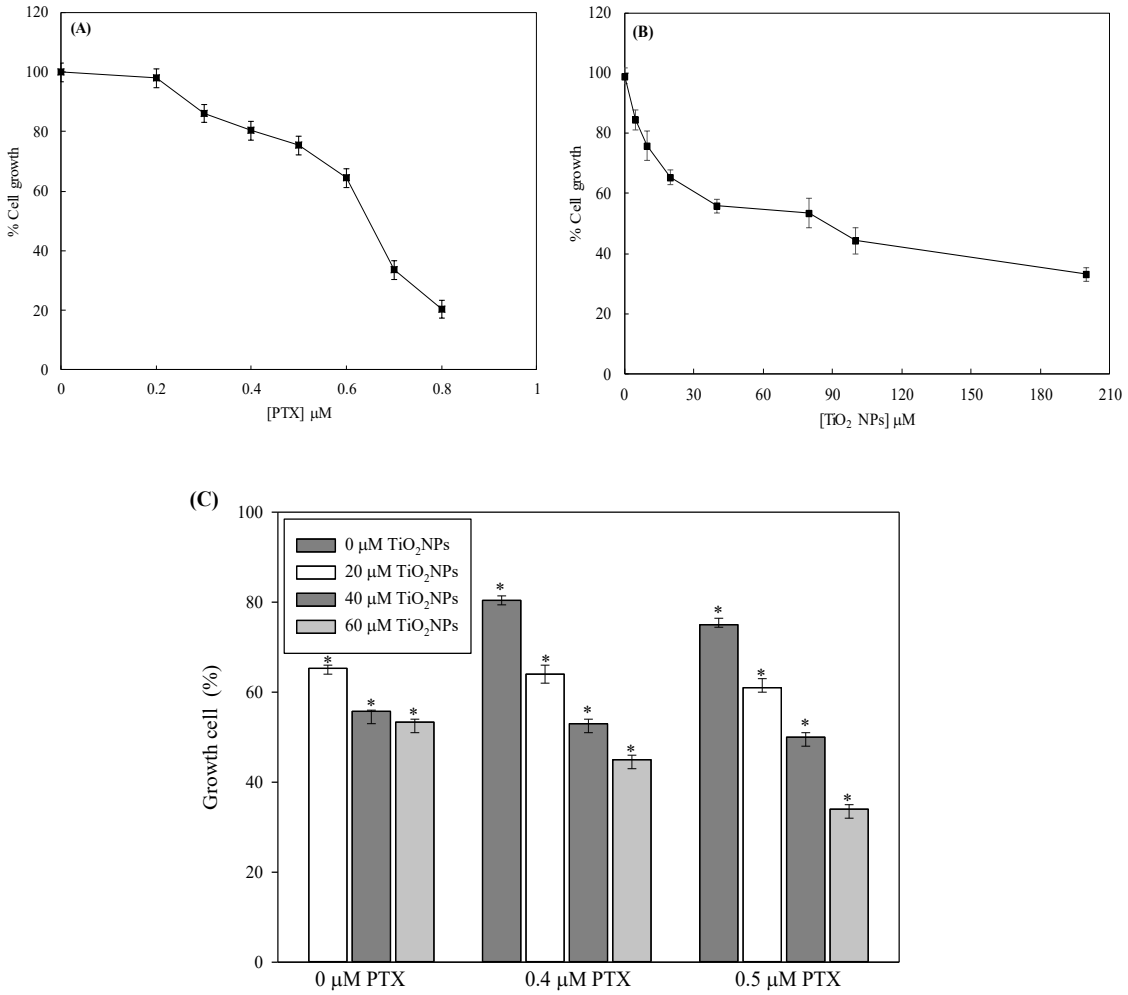

Fig. 6. MTT assay after 48 h. The antiproliferative effects of: (A) varying concentrations of PTX and (B) varying concentrations of TiO_2NPs on MDA-MB-231. (C) The cell growth (%) of 0.4 and 0.5 µM PTX with 20, 40 and 60 µM TiO_2NPs. The data are obtained from the Means of three independent measurements ± SD (*P < 0.05 compared to untreated control cells).

of λ_{max} including hypochromic, hyperchromic, hypsochromic (blue-shift), and bathochromic (red-shift). After the addition of TiO_2NPs to DNA+PTX solution hyperchromic in absorbance occurred and was along with a hypsochromism in λ_{max}, which shows the interaction between TiO_2NPs to DNA+PTX. The hyperchromic effect occurring in DNA can be affiliated to the feature of the excitonic states, which are more delocalized in the single-stranded conditions, at least in the frequency window of the λ_{max}. Such states display an enhanced absorbance [19]. This type of behavior also displays the alteration in DNA conformation upon interaction with ligands. It is described in the literature that hyperchromism results from DNA structure secondary damage and the extent of the hyperchromism are indicative of partial or non-intercalative binding types [20]. Consequently, the UV results indicated that at 46.5 µM of TiO_2NPs or 160 µM of PTX, the 8.32 µM DNA solution was saturated. However, in the present of 60 µM PTX and 15.5 µM TiO_2NPs the DNA solution was saturated. Altogether, our measurements suggested that the structure of DNA molecule in the presence of PTX in combination with TiO_2NPs changed significantly rather than TiO_2NPs or PTX alone. When a fixed amount of TiO_2NPs was added to PTX (Fig. 2D), a rising trend in λ_{max} of PTX was found. The above evidence is indicative of the formation of some type of PTX-TiO_2NPs complex

[1, 15]. Consequently, it is possible for TiO_2NPs bind to the free PTX in solution. However, it should be noted that in this research, we just add PTX and TiO_2NPs in DNA solution.

Fluorescence spectroscopy is one of the electromagnetic spectroscopies that offers information about the configuration, the binding location, the solvent interactions, and the intra-molecular distances of macromolecules. Small ligands can bind to DNA helix via diverse binding modes: groove binding, electrostatic binding, and intercalative binding. The fluorescence intensity of DNA is also weak. Consequently, the DNA-ligand binding cannot be attained through the emission spectra directly. Hence, competitive ligand binding experiments have been done to acquire the binding affinity of TiO_2NPs, PTX, and TiO_2NPs+PTX with DNA. Although, the fluorescence of EtBr (a typical DNA probes) is weak, its fluorescence emission in the presence of DNA increment remarkably. With increasing concentrations of TiO_2NPs, the intensity of DNA-EtBr was diminished without any shifts in fluorescence $\lambda_{max,em}$ (Fig. 3A), which might be attributable to the three possible reasons. First, TiO_2NPs might replace with EtBr in the complex and decreased the EtBr concentration binding to DNA molecule, namely after adding TiO_2NPs to the DNA-EtBr solution, some EtBr molecules were released into solution after an exchange with TiO_2NPs, and fluorescence quenching occurred [21, 22]. Second, TiO_2NPs might be bind to the EtBr causing fluorescence quenching. Third, a new complex between TiO_2NPs and DNA-EtBr was formed. The K_A of DNA-EtBr system was found to be 5.16×10^5 M^{-1} [23]. The smaller K_A between DNA and TiO_2NPs (8.0×10^2 M^{-1}) suggesting that the replacement of EtBr from DNA was not possible. The EtBr fluorescence intensity does not modify much more upon TiO_2NPs addition (Fig. 3A) demonstrating that TiO_2NPs could not interact with EtBr. As a result, TiO_2NPs might interact with the DNA-EtBr complex by way of groove binding or electrostatic interactions [15, 24]. Through increasing the concentration of PTX, gradual fluorescence quenching took place with no shifts in fluorescence $\lambda_{max,em}$ (Fig. 3B). Our observation is in agreement with fluorescence quenching behavior that was reported for Taxol-DNA interaction [25]. Through increasing the concentration of TiO_2NPs to DNA-EtBr-PTX solution fluorescence quenching took place with no shifts in fluorescence $\lambda_{max,em}$. The smaller binding constants (4.0×10^3 M^{-1} and 2.1×10^4 M^{-1}) between TiO_2NPs and DNA-EtBr-PTX suggesting that replacement of EtBr from DNA was not possible. As a result, TiO_2NPs might interact with the DNA-EtBr complex by way of groove binding or electrostatic interactions [13, 23]. It is important to mention that, in the TiO_2NPs and PTX highest concentration the solutions remained clear.

Fluorescence quenching means any process wherein the fluorescence emission of a given fluorophore reduces after adding quencher [11]. Quenching can arise via different molecular mechanisms: molecular rearrangement, collisional quenching (dynamic quenching), ground state complex formation (static quenching), and energy transfer [1]. It is possible to evaluate the quenching rate parameters via Stern-Volmer plots by using fluorescence quenching data. With the Stern-Volmer plot for titration of DNA-bound EtBr with PTX, we have calculated $K_{SV1,}$ $K_{SV2,}$ k_{q1} and k_{q2}, i.e. DNA has two binding constants for PTX. The values of K_{sv} are comparable with K_{sv} of most of the groove binders. Consequently, proposing the groove binding mode chance of PTX with DNA [26]. Using Eq. 2, a linear plot for F_0/F versus [PTX] was achieved. Because the determined value of k_q is higher than the limiting value of 1×10^{10} M^{-1} s^{-1} [27], the fluorescence quenching mechanism is more static rather than dynamic collision. Furthermore, the K_{SV} for DNA-EtBr with PTX decreases after incrementing temperature from 27 to 37 °C (Fig. 3B). This phenomenon displays that the fluorescence quenching process is static, i.e. the non-fluorescent complexes are formed between PTX and DNA [26]. In contrast, we achieved a positive deviation for the plots of F_0/F versus [TiO_2NPs]. Hence, the TiO_2NPs binding to DNA-EtBr and DNA-EtBr-PTX possibly initiated via non-fluorescence complex formation (static quenching) [27].

The K_A and n for static quenching were determined (Table 1). From the viewpoint of the molecular population, it could be explained that when the temperature is increased, consistent with the Boltzmann distribution law, the higher energy molecular levels are occupied. Consequently, the possibility of the ligands and DNA interaction is increased and the values of K_A are also increased [28]. As indicated in Table 1, two types of binding were detected for PTX-DNA and TiO_2NPs-PTX-DNA. This data is in agreement with the earlier study [6]. Furthermore, one binding site was detected in DNA-TiO_2NPs complex. It should be stated that in

the biological systems it is typical that the value of *n* involves more than one binding site [29]. In our experiments, the value of *n* was about equal to 1 for TiO_2NPs (Table 1), suggesting that TiO_2NPs binds to DNA, forming 1:1 adduct. Also, it can be suggested the existence of two classes of binding sites for DNA+PTX and DNA+PTX+TiO_2NPs. Additionally, it can be found from these data that the *n* values for DNA+PTX+TiO_2NPs differ from DNA+TiO_2NPs and DNA+PTX. This result proposes that the molecular population of these different systems contribute not equally in molecular interactions in PTX, TiO_2NPs or PTX-TiO_2NPs with DNA [30]. The order of binding constants of TiO_2NPs, PTX and PTX+TiO_2NPs with DNA was as follows:

K_A (DNA+PTX+TiO_2NPs) > K_A (DNA+PTX) > K_A (DNA+TiO_2NPs)

An enhance in the amount of K_A in the presence of PTX+TiO_2NPs suggested an increasing binding tendency of titanium dioxide nanoparticles and paclitaxel to DNA in comparison with TiO_2NPs and PTX alone. In consequence, PTX+TiO_2NPs may damage DNA structure more efficiently compared to either PTX or TiO_2NPs alone.

To acquire a piece of information about the interaction in-depth, the approach of analyzing the $\Delta G°$ into component terms is a powerful method. The great negative values of $\Delta G°$ point out that TiO_2NPs, PTX, and PTX+TiO_2NPs interaction to DNA was all spontaneously. Comparison of the ΔG° exposes that PTX in combination with TiO_2NPs was more favorable to bind to DNA and the complex formed between PTX+TiO_2NPs and DNA was more stable [31].

Calculation of the thermodynamic parameters is very useful for approving the binding force. The acting forces among a ligand and a macromolecule generally include hydrophobic force, hydrogen bond, van der Waals force, and electrostatic force [32]. The positive ΔH° and ΔS° values specified that hydrophobic force has an essential part in the interaction of TiO_2NPs, PTX, and PTX+TiO_2NPs with DNA [11]. It can be realized that the DNA-binding process is endothermic for PTX+TiO_2NPs and has a large positive entropy value. The positive value of ΔS° is regularly regarded as hydrophobic interaction evidence due to the fact that the water molecules that are organized in an orderly way around the PTX+TiO_2NPs and DNA obtain a more random configuration [33, 34].

Circular dichroism is a spectroscopic technique, which can estimate the alternations of DNA helix with diverse concentrations of NPs. The CD spectra investigations displayed that PTX (60 μM) in combination with TiO_2NPs has an influence on the right-handed chiral structure and the DNA base stacking. Amusingly, the effects of PTX (160 μM) on DNA base stacking is equal to 15.5 μM titanium dioxide nanoparticles+60 μM paclitaxel. Despite the fact, PTX disturbs both right-handed helicity and base stacking of DNA simultaneously. However, PTX modification degree is not strong compared with that of PTX+TiO_2NPs. Furthermore, after the addition of PTX+TiO_2NPs, an augmentation in negative molar ellipticity is observed at 245 nm. The variation in elliptical at 245 nm and 275 nm bands could be attributable to the structural transition in DNA from its native form (B-type) to C-type [35]. More importantly, once B-form to C-form transition happens, the CD band at 245 nm displays about a 66% reduction in its intensity [35, 36]. Hence, it could be concluded that after the addition of PTX+TiO_2NPs, DNA duplex assumes a transitional state having features of both B and C conformation. Similar results have been observed previously [35, 36]. Consequently, PTX+TiO_2NPs can cause a disturbance in the DNA conformation. Moreover, it has been proven that the amount of the elliptical component at 275 nm has a correlation with the winding angle of DNA, i.e., the reduction in its magnitude generates an increment in winding angle. Additionally, any enhancement in DNA winding angle could be an indication of DNA groove widening as a result of the positioning of TiO_2NPs and PTX within a DNA groove pocket [36]. In summary, PTX in combination with TiO_2NPs modify DNA structure by a simple and reasonable mechanism: change in DNA conformation from B to C-form. However, future experiments must be done to determine the underlying mechanisms. This observation demonstrates good agreement with studies of UV absorption and fluorescence emission as mentioned above.

The most important reference about the particle surface charge in a colloidal solution is the zeta potential value, which can be measured via various techniques. The ζ potential or charge density is a physical characteristic that is demonstrated by any particle in suspension. ζ potential is the particle surface electrical charge measurement. The ζ potential investigations approved that PTX+TiO_2NPs interact with DNA molecule and

during this interaction, some of the negatively charged DNA phosphate groups have been neutralized via PTX+TiO_2NPs [37]. The higher reduction in DNA negative charge in the presence of titanium dioxide nanoparticles and paclitaxel established that backbone binding was the major binding force [38]. Our result is in agreement with Ouameur *et. al.* experiments, who have indicated that taxol binds to DNA at AT, GC bases, and the PO_2 group of DNA backbone. The neutralization at the DNA backbone decreases the inter- and intra-strand electrostatic repulsions present in the native DNA phosphate backbone [39]. Moreover, neutralizing the DNA phosphate groups can diminish the repulsion across the minor groove, therefore the minor groove becomes narrower [40]. Consequently, the main purpose of our study is that with the aid of TiO_2NPs, PTX (in lower concentration) can significantly disturb the DNA conformation compared to that of TiO_2NPs or PTX alone, i.e. at a lower concentration of PTX (60 µM, concentration at the half-saturation of DNA+PTX) in combination of TiO_2NPs (15.5 µM) more structural effects detected than PTX (160 µM) or TiO_2NPs (46.5 µM) alone. In another word, PTX and TiO_2NPs can cooperatively alter the structure of DNA, which is the goal of our study. So even though TiO_2NPs exhibited lower structural changes on DNA conformation but when we combined it with PTX more structural effects were observed.

As we know cytotoxicity tests of a new nano-drug is the first-level evaluation before biomedical applications. Therefore, we have performed the MTT assay to determine the antiproliferative effects exerted by TiO_2NPs, PTX, and PTX+TiO_2NPs on the MDA-MB-231 breast cancer cell line. As exposed in Fig. 6A, B, TiO_2NPs alone and PTX alone reduced the viability of MDA-MB-231 cells. Furthermore, it is clear that PTX alone and TiO_2NPs alone made dose-response suppression on the growth of MDA-MB-231 cells. Accordingly, the IC_{50} of PTX alone and TiO_2NPs alone were determined to be 0.65 and 90 µM. In the follow-up experiment, by the use of MTT assay, PTX was employed at the concentrations of 0.4 µM and 0.5 µM, combined with TiO_2NPs at the concentrations of 20, 40, and 60 µM to attain the optimum combination condition that affected the majority of MDA-MB-231 cells (Fig. 6C). It is important to note that the selected concentrations of PTX and TiO_2NPs were lower than the IC_{50} of the MDA-MB-231 cells [1]. It was discovered that PTX combined with TiO_2NPs could inhibit cell proliferation remarkably and 60 µM TiO_2NPs achieved the best inhibition of MDA-MB-231cell growth (Fig. 6C). As shown in Fig. 6, using the selected concentrations of PTX (0.4 µM and 0.5 µM), less than 25% cell death happened (about 75% cell growth occurred). Using the selected concentrations of TiO_2NPs (20, 40, and 60 µM), less than 45% cell death occurred (55% cell growth occurred). Conversely, cell death increased to 62% (38% cell growth occurred) when 0.5 µM PTX was utilized in the presence of 60 µM TiO_2NPs. Based on these observations, it seemed that PTX combined with TiO_2NPs could promote the mortality of cells besides those mortality effects induced via PTX or TiO_2NPs alone. Our study can provide a novel strategy for designing the ideal PTX formulation with lower side effects. It is hoped that any information from this study provides tangible benefits to patients in terms of both survival and life quality.

CONCLUSION

This investigation proved that the presence of TiO_2NPs could improve the effects of PTX on the DNA molecule configuration and increase the affinity of PTX to DNA. Consequently, the existence of synergism between titanium dioxide nanoparticles and paclitaxel was shown in this research. We also proved that the presence of TiO_2NPs could improve the cytotoxic effect of PTX on MDA-MB-231 cells (the triple-negative breast cancer cell line), having a significant difference with PTX alone or TiO_2NPs alone. Although further investigations are required, this study can provide a novel strategy for designing the ideal PTX formulation. It is expected that all information from this research could offer obvious advantages for patients in terms of both life quality and survival.

ACKNOWLEDGMENTS

We thank Ms. Evini at the Institute of Biochemistry and Biophysics of the University of Tehran for technical support.

CONFLICT OF INTEREST

The authors declare that there is no conflict of interests regarding the publication of this manuscript.

REFERENCES

1. Hekmat A, Saboury A, Divsalar A, Seyedarabi A. Structural

Effects of TiO2 Nanoparticles and Doxorubicin on DNA and their Antiproliferative Roles in T47D and MCF7 Cells. Anti-Cancer Agents in Medicinal Chemistry. 2013;13(6):932-51.
2. Disdier C, Chalansonnet M, Gagnaire F, Gaté L, Cosnier F, Devoy J, et al. Brain Inflammation, Blood Brain Barrier dysfunction and Neuronal Synaptophysin Decrease after Inhalation Exposure to Titanium Dioxide Nano-aerosol in Aging Rats. Scientific Reports. 2017;7(1).
3. Shukla RK, Kumar A, Gurbani D, Pandey AK, Singh S, Dhawan A. TiO2nanoparticles induce oxidative DNA damage and apoptosis in human liver cells. Nanotoxicology. 2011;7(1):48-60.
4. Shi H, Magaye R, Castranova V, Zhao J. Titanium dioxide nanoparticles: a review of current toxicological data. Particle and Fibre Toxicology. 2013;10(1):15.
5. Sofias AM, Dunne M, Storm G, Allen C. The battle of "nano" paclitaxel. Advanced Drug Delivery Reviews. 2017;122:20-30.
6. Ouameur AA, Malonga H, Neault JF, Diamantoglou S, Tajmir-Riahi HA. Taxol interaction with DNA and RNA Stability and structural features. Canadian Journal of Chemistry. 2004;82(6):1112-8.
7. Kaelin WG. The Concept of Synthetic Lethality in the Context of Anticancer Therapy. Nature Reviews Cancer. 2005;5(9):689-98.
8. Lehár J, Krueger AS, Avery W, Heilbut AM, Johansen LM, Price ER, Rickles RJ, Short Iii GF, Staunton JE, Jin X. Synergistic drug combinations tend to improve therapeutically relevant selectivity. Nature biotechnology. 2009;27:659.
9. Venkatasubbu GD, Ramasamy S, Reddy GP, Kumar J. In vitro and In vivo anticancer activity of surface modified paclitaxel attached hydroxyapatite and titanium dioxide nanoparticles. Biomedical Microdevices. 2013;15(4):711-26.
10. Hekmat A, Salavati F, Tackallou SH. The Effects of Paclitaxel in the Combination of Diamond Nanoparticles on the Structure of Human Serum Albumin (HSA) and Their Antiproliferative Role on MDA-MB-231cells. The Protein Journal 2020; 39(3):268.
11. Shahabadi N, Maghsudi M. Multi-spectroscopic and molecular modeling studies on the interaction of antihypertensive drug; methyldopa with calf thymus DNA. Mol BioSyst. 2014;10(2):338-47.
12. Park IK, Kim TH, Park YH, Shin BA, Choi ES, Chowdhury EH, et al. Galactosylated chitosan-graft-poly(ethylene glycol) as hepatocyte-targeting DNA carrier. Journal of Controlled Release. 2001;76(3):349-62.
13. Koch D, Manzhos S. On the Charge State of Titanium in Titanium Dioxide. The Journal of Physical Chemistry Letters. 2017;8(7):1593-8.
14. Patel S, Patel P, Undre SB, Pandya SR, Singh M, Bakshi S. DNA binding and dispersion activities of titanium dioxide nanoparticles with UV/vis spectrophotometry, fluorescence spectroscopy and physicochemical analysis at physiological temperature. Journal of Molecular Liquids. 2016;213:304-11.
15. Markeb AA, El-Maali NA, Sayed DM, Osama A, Abdel-Malek MAY, Zaki AH, et al. Synthesis, Structural Characterization, and Preclinical Efficacy of a Novel Paclitaxel-Loaded Alginate Nanoparticle for Breast Cancer Treatment. International Journal of Breast Cancer. 2016;2016:1-8.
16. Rehman SU, Sarwar T, Husain MA, Ishqi HM, Tabish M. Studying non-covalent drug–DNA interactions. Archives of Biochemistry and Biophysics. 2015;576:49-60.
17. Vujčić MT, Tufegdžić S, Novaković I, Djikanović D, Gašić MJ, Sladić D. Studies on the interactions of bioactive quinone avarone and its methylamino derivatives with calf thymus DNA. International Journal of Biological Macromolecules. 2013;62:405-10.
18. Bischoff G, Gromann U, Lindau S, Meister WV, Hoffmann S. A Spectroscopic and Thermodynamic Study of Taxol Nucleic Acid Complexes. Nucleosides and Nucleotides. 1999;18(10):2201-17.
19. D'Abramo M, Castellazzi CL, Orozco M, Amadei A. On the Nature of DNA Hyperchromic Effect. The Journal of Physical Chemistry B. 2013;117(29):8697-704.
20. Awasthi P, Kumar N, Kaushal R, Kumar M, Kukreti S. ComparativeIn VitroBinding Studies of TiCl2(dpme)2, Ti(ada)2(bzac)2, and TiCl2(bzac)(bpme) Titanium Complexes with Calf-Thymus DNA. Biochemistry Research International. 2015;2015:1-7.
21. Shahabadi N, Hakimi M, Morovati T, Fatahi N. DNA binding affinity of a macrocyclic copper(II) complex: Spectroscopic and molecular docking studies. Nucleosides, Nucleotides and Nucleic Acids. 2017;36(8):497-510.
22. Hekmat A, Saboury AA, Divsalar A. The Effects of Silver Nanoparticles and Doxorubicin Combination on DNA Structure and Its Antiproliferative Effect Against T47D and MCF7 Cell Lines. Journal of Biomedical Nanotechnology. 2012;8(6):968-82.
23. Ramana MMV, Betkar R, Nimkar A, Ranade P, Mundhe B, Pardeshi S. Synthesis of a novel 4H-pyran analog as minor groove binder to DNA using ethidium bromide as fluorescence probe. Spectrochimica Acta Part A: Molecular and Biomolecular Spectroscopy. 2016;152:165-71.
24. Geng S, Liu G, Li W, Cui F. Molecular interaction of ctDNA and HSA with sulfadiazine sodium by multispectroscopic methods and molecular modeling. Luminescence. 2013;28(5):785-92.
25. Krishna AG, Kumar DV, Khan BM, Rawal SK, Ganesh KN. Taxol–DNA interactions: fluorescence and CD studies of DNA groove binding properties of taxol. Biochimica et Biophysica Acta (BBA) - General Subjects. 1998;1381(1):104-12.
26. Mukherjee A, Singh B. Binding interaction of pharmaceutical drug captopril with calf thymus DNA: a multispectroscopic and molecular docking study. Journal of Luminescence. 2017;190:319-27.
27. Masters BR. Principles of fluorescence spectroscopy. Journal of Biomedical Optics. 2008;13:029901.
28. Jafari F, Samadi S, Nowroozi A, Sadrjavadi K, Moradi S, Ashrafi-Kooshk MR, et al. Experimental and computational studies on the binding of diazinon to human serum albumin. Journal of Biomolecular Structure and Dynamics. 2017;36(6):1490-510.
29. Moradi SZ, Nowroozi A, Sadrjavadi K, Moradi S, Mansouri K, Hosseinzadeh L, et al. Direct evidences for the groove binding of the Clomifene to double stranded DNA. International Journal of Biological Macromolecules. 2018;114:40-53.
30. Khan S, Malla AM, Zafar A, Naseem I. Synthesis of novel coumarin nucleus-based DPA drug-like molecular entity:

In vitro DNA/Cu(II) binding, DNA cleavage and pro-oxidant mechanism for anticancer action. PLOS ONE. 2017;12(8):e0181783.
31. Li S, Pan J, Zhang G, Xu J, Gong D. Characterization of the groove binding between di-(2-ethylhexyl) phthalate and calf thymus DNA. International Journal of Biological Macromolecules. 2017;101:736-46.
32. Hekmat A, Saboury AA, Moosavi-Movahedi AA, Ghourchian H, Ahmad F. Effects of pH on the activity and structure of choline oxidase from Alcaligenes species. Acta Biochimica Polonica. 2008;55(3):549-57.
33. Xu L, Hu Y-X, Li Y-C, Zhang L, Ai H-X, Liu Y-F, et al. In vitro DNA binding studies of lenalidomide using spectroscopic in combination with molecular docking techniques. Journal of Molecular Structure. 2018;1154:9-18.
34. Moradi Z, Khorasani-Motlagh M, Rezvani AR, Noroozifar M. Evaluation of DNA, BSA binding, and antimicrobial activity of new synthesized neodymium complex containing 29-dimethyl 110-phenanthroline. Journal of Biomolecular Structure and Dynamics. 2017;36(3):779-94.
35. Ray B, Agarwal S, Lohani N, Rajeswari MR, Mehrotra R. Structural, conformational and thermodynamic aspects of groove-directed-intercalation of flavopiridol into DNA. Journal of Biomolecular Structure and Dynamics. 2016;34(11):2518-35.
36. Agarwal S, Jangir DK, Mehrotra R, Lohani N, Rajeswari MR. A Structural Insight into Major Groove Directed Binding of Nitrosourea Derivative Nimustine with DNA: A Spectroscopic Study. PLoS ONE. 2014;9(8):e104115.
37. Veeralakshmi S, Nehru S, Sabapathi G, Arunachalam S, Venuvanalingam P, Kumar P, et al. Single and double chain surfactant–cobalt(iii) complexes: the impact of hydrophobicity on the interaction with calf thymus DNA, and their biological activities. RSC Advances. 2015;5(40):31746-58.
38. Ghosh D, Dey SK, Saha C. Mutation Induced Conformational Changes in Genomic DNA from Cancerous K562 Cells Influence Drug-DNA Binding Modes. PLoS ONE. 2014;9(1):e84880.
39. Bhattacharya S, Mandal SS. Interaction of surfactants with DNA. Role of hydrophobicity and surface charge on intercalation and DNA melting. Biochimica et Biophysica Acta (BBA) - Biomembranes. 1997;1323(1):29-44.
40. Hamelberg D, Williams LD, Wilson WD. Effect of a neutralized phosphate backbone on the minor groove of B-DNA: molecular dynamics simulation studies. Nucleic acids research. 2002;30:3615.